# Quantum-chemical study of excitons in tetragonal $BaTiO_3$ and $SrTiO_3$ crystals

Ricardo Viteri[a,b,c], Luis Miguel Prócel[a,b], Francisco Tipán[b], Diego Fernando Ortiz[a], Arvids Stashans*[a,b]

[a]Centro de Investigación en Física de la Materia Condensada, Corporación de Física Fundamental y Aplicada, Apartado 17-12-637, Quito, Ecuador
[b]Departamento de Química, Colegio Politécnico, Universidad San Francisco de Quito, Apartado 17-12-841, Quito, Ecuador
[c]Department of Chemistry and Biochemistry, University of Oklahoma, Room 208, 620 Parrington Oval, Norman, Oklahoma 73019, U.S.A.

## ABSTRACT

Using a quantum-chemical INDO method based on the Hartree-Fock formalism and the periodic large unit cell (LUC) model we present a theoretical interpretation of the structural and electronic properties of triplet excitons in the tetragonal $BaTiO_3$ and $SrTiO_3$ crystals. Our study demonstrates that the exciton structure has particularities in each material. In the $BaTiO_3$ the defect structure corresponds to the so-called Mott-Wannier-type exciton having a considerable separation, 7.0 Å, between the hole and the electron. Meanwhile, in $SrTiO_3$ the structural and electronic features of the triplet exciton are quite different. The hole-electron distance is about 2.14 Å and the defect is well localized in two contiguous atoms: the hole on one of the O atoms and the electron on the neighbor Ti atom. The calculated luminescence energy using the so-called ΔSCF method is found to be equal to 0.94 eV and 1.13 eV for $BaTiO_3$ and $SrTiO_3$, respectively. Since it falls within the infrared part of the spectrum, the experimentally detected green luminescence due to photo-excited states should be attributed to the singlet excitons.

**Keywords:** $BaTiO_3$, $SrTiO_3$, excitons, LUC, structural and electronic properties, luminescence

## 1. INTRODUCTION

Barium titanate ($BaTiO_3$) and strontium titanate ($SrTiO_3$) are the most important perovskite-type titanates due to their wide range of applications as electronic materials. The primitive unit cell of $BaTiO_3$ and $SrTiO_3$ contain five atoms[1] similar to other perovskite-type crystals. Although both titanates have similar structure, they exhibit different physical, chemical and electronic properties. Technologically, these differences yield in use of these two materials in different applications. Among a number of important features, $BaTiO_3$ has large electro-optic coefficients and high photorefractive sensivity.[2] This material also can be used in self-pumped phase conjugation or holographic storage[3] and inexpensive diode lasers.[4] Other important properties are its chemical and mechanical stability in a wide temperature range, which facilitates its fabrication in bulk polycrystals and both epitaxial and polycrystalline thin films.[5] Meanwhile, $SrTiO_3$ is used as a grain-boundary barrier layer capacitor, oxygen-gas sensor, epitaxial growth substrate for high-temperature superconductor thin films and catalytic material. $SrTiO_3$ has also been known to become superconducting when a small number of electron carriers are doped by La substitution for a Sr atom[6] (see references therein).

The structures of both barium and strontium titanates have simple cubic symmetry, which transform to the tetragonal ones below the characteristic transition temperature of the material. For $BaTiO_3$ the transition occurs below 380 K while $SrTiO_3$ does transform to tetragonal phase below 105 K. This corresponds to the transition: paraelectric phase → ferroelectric phase. The static dielectric constant increases extraordinarily when the temperature decreases, e.g. $SrTiO_3$ is stabilized at over $10^4$ below 10 K without a ferroelectric phase transition.[7] This property is known as quantum paraelectricity (QPE). The nature of QPE has not yet been revealed.[8] Despite the fact that many studies have been done so far on these ferroelectric materials, there is still no sufficient understanding of the nature of many properties and phenomena in both barium and strontium titanates. On the other hand, it is well understood that point defects play an important role in many applications of $BaTiO_3$ and $SrTiO_3$ crystals and therefore, further studies are necessary on this subject. One of the most common defects in non-metallic crystals is the so-called exciton. Free excitons created by exciting radiation undergo transformation into self-trapped excitons in singlet or triplet states. Later on the recombination between electrons and trapped holes causes the

appearance of the recombination luminescence of the self-trapped exciton. Some considerable efforts have been done to understand the nature of excitons in many oxides. As an example we can note that the adiabatic potential surface for triplet exciton self-trapping has been studied in the $SiO_2$ crystal[9] using the same computer code as we do. The results interpreted in great detail the nature of the self-trapped-exciton optical absorption and luminescence in the $SiO_2$ crystal.[9]

There are not many studies on excitons in perovskites due to the complexity of possible spatial configurations of the exciton in these materials and necessity to take into consideration rather complex chemical bonding, which includes also a covalent component. However, recently quantum-chemical calculations on self-trapped excitons in $KTaO_3$ and $KNbO_3$ crystals have been performed[10] using again the same computer code. Thus, it has been showed repeatedly that the CLUSTERD computer code[11] is adequate for the exciton studies in different oxides. Additionally, we have tested the present method in a number of other applications on titanates. Some examples include studies of hole self-trapping in a pure[12] and defective $BaTiO_3$ crystals,[13] hole self-trapping studies in the $SrTiO_3$ cubic lattice,[14,15] structural and electronic features of triplet excitons in the tetragonal $BaTiO_3$ crystal[16] and defect doping studies in the bulk of $SrTiO_3$,[6,17,18] $CaTiO_3$,[19] $BaTiO_3$,[20,21] $PbTiO_3$[22] crystals as well as quantum-chemical computations of defects on the $SrTiO_3$ surfaces.[23,24]

The purpose of the present article is to obtain equilibrium geometry and electronic structure of the triplet exciton in both $BaTiO_3$ and $SrTiO_3$ tetragonal lattices. Since these materials have different physical, chemical and electronic properties, the geometry and the electronic structure of triplet excitons in these crystals are expected to be different. We also study the lattice distortion due to the exciton and possible luminescence due to the hole-electron pair annihilation.

## 2. OUTLINE OF THE COMPUTATIONAL METHOD

The employed method of periodically repeated large unit cells (LUCs)[9] is designed for the calculation of the total energy

**Table 1.** Numerical parameter sets used in the present work: $\zeta$, $E_{neg}$, $P^0$ and $\beta$.

| Atom | AO | $\zeta$ (au) | $E_{neg}$ (eV) | $P^0$ (e) | $\beta$ (eV) |
|---|---|---|---|---|---|
| Ba | 6s | 1.65 | 11.34 | 0.2 | -0.4 |
| | 5p | 2.8 | 30.6 | 2.0 | -4.0 |
| Ti | 4s | 1.4 | 1.4 | 0.65 | -0.5 |
| | 4p | 1.1 | -10.0 | 0.04 | -0.5 |
| | 3d | 1.93 | -2.9 | 0.62 | -9.0 |
| O | 2s | 2.27 | 4.5 | 1.974 | -16.0 |
| | 2p | 1.86 | -12.6 | 1.96 | -16.0 |
| Sr | 5s | 1.59 | 11.15 | 0.18 | -0.4 |
| | 4p | 2.80 | 37.5 | 2.00 | -4.5 |

and electronic structure of crystals. The calculations are based on the Hartree-Fock formalism in the framework of the intermediate neglect of differential overlap (INDO) approach. We chose the LUC model because of its advantage compared to different cluster models, for example, better treatment of the exchange interaction. Additionally, it is important to note that from the viewpoint of simulating the exciton self-trapping, the original equivalency of the perfect lattice sites is essential. Only the periodic models meet this condition. A full discussion of the mathematical equations to calculate the total energy within the framework of the LUC approach is given in numerous works[9,11,19] carried out before. Here we shall only state that the method includes a number of the so-called semi-empirical parameters. The atomic parameter sets are optimized by calculating the following properties and comparing them to the experimental results: (i) the main features of a given crystal (width of the forbidden energy gap, widths of the upper and lower valence bands, lattice constants of the

crystal), (ii) the inter-atomic distances and ground states of some selected diatomic molecules, and finally (iii) the ionization potentials of the host atoms of the crystal. The numerical parameters for the $BaTiO_3$ and $SrTiO_3$ crystals were obtained before reproducing the most important properties of this material and also in studies of other crystals.

Specifically, the numerical parameter sets for the Ba, O and Ti atoms used in the present work were taken from Ref. 20 while the parameters for Sr 5s and 4p AOs from Ref. 18. Thus, we have restricted ourselves to use the so-called valence basis set. The INDO parameters utilized in the present work are given in Tables 1 and 2. Throughout the present work we have exploited a LUC of 135 atoms, i.e., a 27 times (3x3x3) extended primitive unit cell has been used for both barium and strontium titanates. In order to answer the question of the exciton possible localization/delocalization we have performed the total spin density analysis.

**Table 2.** Electron-core interaction parameters $\alpha_{\mu B}$ for the tetragonal phase. The $\mu$*th* AO belongs to atom A, where A ≠ B.

| | $\alpha_{\mu B}$ ($au^{-1}$) | | | |
|---|---|---|---|---|
| **A** | **B** = Ba | **B** = Ti | **B** = O | **B** = Sr |
| Ba | 0.20 | 0.52 | 0.33 | - |
| Ti | 0.11 | 0.13 | 0.10 | 0.10 |
| O | 0.52 | 0.36 | 0.15 | 0.59 |
| Sr | - | 0.55 | 0.25 | 0.15 |

## 3. RESULTS AND DISCUSSION

### 3.1. Structural and electronic features of triplet excitons in the tetragonal $BaTiO_3$ crystal

As a result of the spin density analysis for the 135 atom LUC, the electronic part of the exciton is found to be well localized on the Ti(11) atom while the hole part settles down mainly on O(8) atom (Fig. 1). The elements of the self-consistent-field (SCF) spin density matrix for the atoms situated within the defective region are given in Table 3. As it follows from these data, 94% of the electron is localized on the $3d_{xy}$ AO of the Ti(11) atom while the hole part is mainly found, 84% of localization, on the $2p_x$ AO of the O(8) atom. However, the $2p_x$ AOs of the O(7) and O(9) share also some part of the hole. This particular localization of the hole may correspond to hole resonance structure occurring among the O(7)-O(8)-O(9) atoms. The approximate distance between the two centers is about 7.0 Å. This implies that we have the so-called Mott-Wannier-type exciton. The exciton is weakly bound, which is a commonly accepted exciton model for the ionic crystals.

The performed geometry optimization leads to a rather strong electronic density re-distribution due to the exciton presence. It is found that the two O(8)-nearest Ti atoms, Ti(5) and Ti(6), situated along the y-axis move outward the O(8) atom by 0.08 Å. The four O(8)-nearest Ba atoms also move outward the defect along the <101> direction by about 0.03 Å. Finally, the two Ti-closest O atoms located along the y-axis, O(7) and O(9), move towards the O(8) atom and thus reduce the chemical bond lengths between Ti(5)-O(7) and Ti(6)-O(9). Considering these particular atomic movements, we have obvious lattice polarization due to the hole presence. This polarization occurs along the y direction and also leads to weakening of the chemical bonding between the oxygen, which receives a hole, and its surrounding cations. It is important to state that the polarization axis does not coincide with the ferroelectric z-axis. Thus one can see that exciton presence in the ferroelectric tetragonal $BaTiO_3$ phase might reduce ferroelectric polarization in this material and can induce the loss of bulk ferroelectricity in the material.

The analysis of the electronic part of the exciton shows that it is well localized on the Ti(11) atom. Again, due to the vicinity polarization effect we observe the atomic movements along the z-axis as shown in Fig. 1. In the present case the lattice polarization is along the ferroelectric axis. However, its direction is opposite, i.e., the induced local polarization due to the

**Fig. 1.** The hole part, O(8) atom, and the electron part, Ti(11) atom, of the exciton and displacements of the neighboring atoms. The positi [illegible] O(8) atom. One can observe the lattice polar [illegible] some polarization along the z axis.

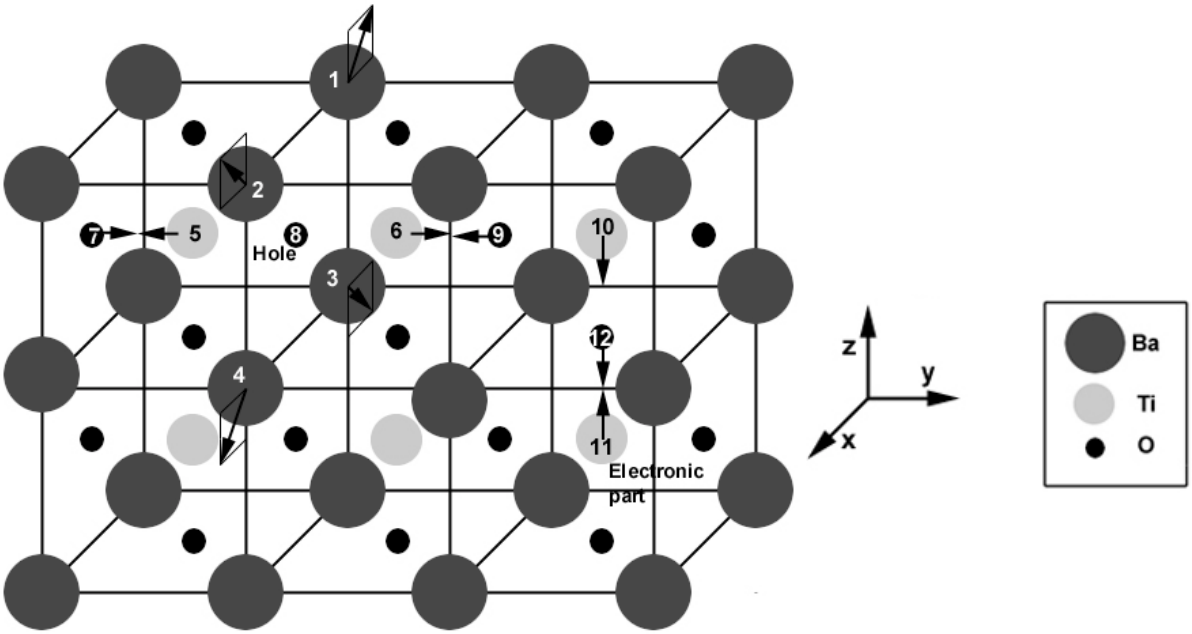


**Table 3.** SCF spin density matrix elements for the atoms within the defective region. Predominantly, the electronic part is localized on the $3d_{xy}$ AO of the Ti(11) atom while the hole part is found to be localized mainly on the $2p_y$ AO of the O(8) atom. The atomic numeration corresponds to the one given in Fig. 1.

| Electron | $4s$ | $4p_x$ | $4p_y$ | $4p_z$ | $3d_{x^2-y^2}$ | $3d_{xy}$ | $3d_{xz}$ | $3d_{yz}$ | $3d_{z^2}$ |
|---|---|---|---|---|---|---|---|---|---|
| Ti(5) | -0.04467 | -0.00122 | -0.00387 | -0.00129 | -0.14112 | -0.01274 | -0.00521 | -0.01584 | -0.05855 |
| Ti(6) | -0.04467 | -0.00122 | -0.00387 | -0.00129 | -0.14112 | -0.01274 | -0.00521 | -0.01584 | -0.05855 |
| Ti(11) | 0.01551 | 0.00268 | 0.0026 | 0.00085 | 0.01772 | **0.93938** | 0.01282 | 0.01228 | 0.03135 |

| Hole | $2s$ | $2p_x$ | $2p_y$ | $2p_z$ |
|---|---|---|---|---|
| O(7) | 0.00394 | 0.00764 | **0.27763** | 0.00921 |
| O(8) | 0.0042 | 0.0052 | **0.85785** | 0.00512 |
| O(9) | 0.00394 | 0.00764 | **0.27763** | 0.00921 |

electron trapping at the Ti(11) atoms reduces the total ferroelectric moment. The calculated relaxation energy as a difference between the total energies of relaxed and unrelaxed systems is found to be equal to 4.4 eV.

### 3.2. Structural and electronic features of triplet excitons in the tetragonal $SrTiO_3$ crystal

As a result of the spin density analysis for the 135 atom LUC, the electronic part of the exciton is found to be well localized on the Ti(4) atom while the hole part settles down on the O(3) atom (Fig. 2). The elements of the SCF spin density matrix for the atoms situated within the defective region are given in Table 4. As it follows from these data 93% of the electron is localized on the $3d_{xy}$ AO of the Ti(4) atom while the hole part mainly is found, 84% of localization, on the $2p_x$ (39%) and $2p_y$ (45%) AOs of the O(3) atom.

**Fig. 2.** Spatial structure of the triplet exciton in the tetragonal $SrTiO_3$ lattice. The hole and the electronic parts are localized on the O(3) and Ti(4) atoms, respectively. The surrounding atoms move outwards the defect along the y axis creating the crystalline lattice polarization along the same axis.

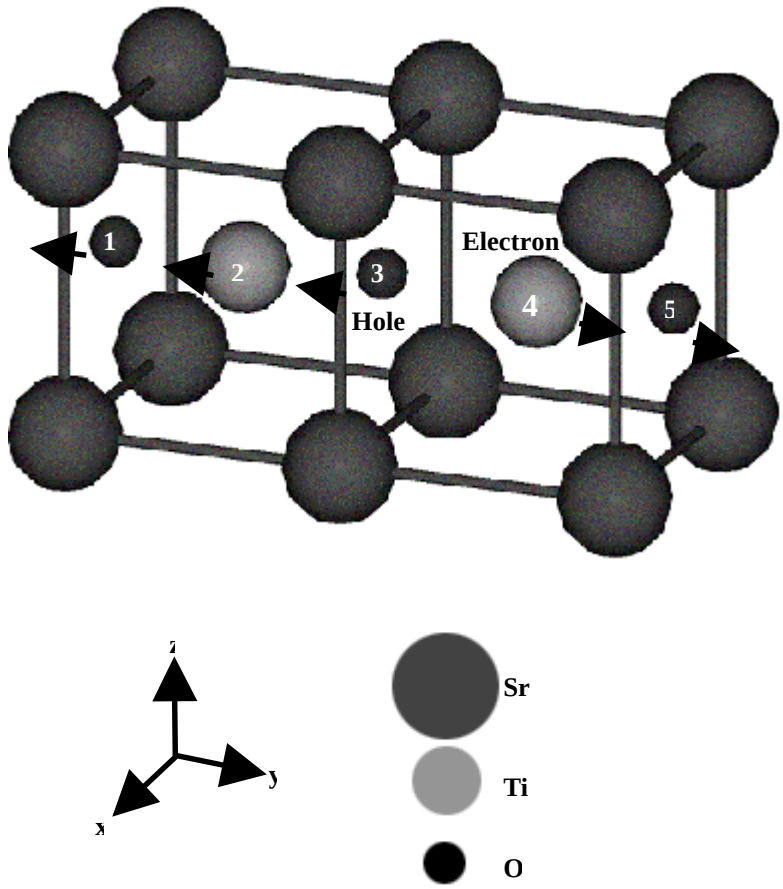


The performed geometry optimization as it is shown in Table 5 leads to rather strong electronic density re-distribution. In general, it is found that the movements of five atoms in the defective region are non-negligible. Two of them move up to 4% (0.15 Å) of the magnitude of the corresponding lattice parameter $a_o$ = 3.88 Å. It should be mentioned that due to the fact that all atomic movements are along the y axis, we express the lattice distortion in terms of the $a_o$ lattice parameter. The defect-nearest O(1), Ti(2) and O(5) atoms, situated along the y-axis, move outwards the defect (see Fig. 2). As one can see from the atomic charge analysis (Table 5) and also considering the above-mentioned particular atomic movements, there exists obvious lattice polarization due to the hole presence. This polarization occurs along the y direction and also leads to a weakening of the chemical bonding between the oxygen, which receives a hole and its surrounding cations. It is important to state that the polarization axis does not coincide with the ferroelectric z-axis similarly as in the case of the $BaTiO_3$ crystal discussed above.

The computed distance between the two centers, hole and electron, is found to be approximately 2.14 Å. This implies that the triplet state exciton in the $SrTiO_3$ crystal is stronger bound compared to the case of the $BaTiO_3$ crystal. Finally, we can state that the calculated relaxation energy is found to be equal to 3.3 eV.

**Table 4.** SCF spin density matrix elements for the atoms within the defective region. Predominantly, the electronic part of triplet exciton is localized on the $3d_{xy}$ AO of the Ti(4) atom while the hole part is found to be localized on the $2p_x$ and $2p_y$ AOs of the O(3) atom. The atomic numeration corresponds to the one given in Fig. 2.

| Electron | $4s$ | $4p_x$ | $4p_y$ | $4p_z$ | $3d_{x^2-y^2}$ | $3d_{xy}$ | $3d_{xz}$ | $3d_{yz}$ | $3d_{z^2}$ |
|---|---|---|---|---|---|---|---|---|---|
| Ti(2) | -0.0396 | -0.0054 | -0.0046 | -0.0014 | -0.0809 | -0.0480 | -0.0092 | -0.0109 | -0.0376 |
| Ti(4) | 0.0053 | 0.0016 | 0.0006 | 0.0003 | 0.0056 | **0.9307** | 0.0134 | 0.0103 | 0.0263 |

| Hole | $2s$ | $2p_x$ | $2p_y$ | $2p_z$ |
|---|---|---|---|---|
| O(1) | 0.0006 | 0.0058 | 0.0649 | 0.0036 |
| O(3) | 0.0044 | **0.3868** | **0.4550** | 0.0090 |
| O(5) | -0.0003 | 0.0000 | 0.0222 | -0.0032 |

**Table 5.** Atomic displacements, Δr, and changes in atomic charge, Δq, due to the triplet exciton self-trapping in the tetragonal $SrTiO_3$ lattice. The atomic numeration and the direction of their movements correspond to the one given in Fig. 2.

| Atom | Δr (% $a_o$) | Δq (e) |
|---|---|---|
| O(1) | 1.0 | +0.096 |
| Ti(2) | 4.0 | -0.280 |
| O(3) | 4.0 | +0.450 |
| Ti(4) | 2.1 | -0.500 |
| O(5) | 2.0 | +0.097 |

### 3.3. Luminescence due to the exciton in $SrTiO_3$ and $BaTiO_3$

Annihilation of an exciton, i.e., electron and hole mutual recombination gives rise to the luminescence, which can be observed experimentally. In our study, the luminescence energy was obtained as a difference of total energies for the self-consistent-field ground and excited states for optimized triplet exciton geometry (ΔSCF method). That is, the potential energy curve was calculated for the triplet exciton, and then according to the Frank-Condon principle the de-excitation energy is that for the vertical transition from the minimum of the triplet exciton relaxed state to the SCF singlet state of the exciton for a fixed atomic arrangement. Thus computed luminescence energy was found to be equal to 0.94 eV for $BaTiO_3$ and 1.13 eV for $SrTiO_3$.

In this connection, some recent results reported for the triplet exciton state in the cubic phase of $ABO_3$ oxides[10,25] should be mentioned. The authors propose the charge-transfer vibronic exciton (CTVE) approach to describe the electronic excitations in these systems. However, they use the electronic density matrix in their analysis of electron and hole polaron localization within the crystalline lattice, rather that the SCF spin density matrix, which gives a more precise pattern for the exciton localization. Secondly, the geometry used in their works apparently does not correspond to the equilibrium geometry

leading to incorrect values of calculated luminescence energies. Therefore, the CTVE existence in titanates is rather doubtful.

Our theoretical interpretation of the results obtained in the present work is given in Fig. 3. In our mind, the experimentally observed green luminescence in a number of perovskites is due to singlet excitons in these materials. Since the triplet state

**Fig. 3.** Total energy curve as a function of the generalized coordinate, Q, for the self-trapped exciton in the tetragonal $BaTiO_3$ and $SrTiO_3$ lattices (energy values in parenthesis correspond to $SrTiO_3$). The luminescence of the singlet state might be responsible for the experimentally detected green light, while the triplet exciton state lies considerably lower and as a result might participate in the photodegradation of the material.

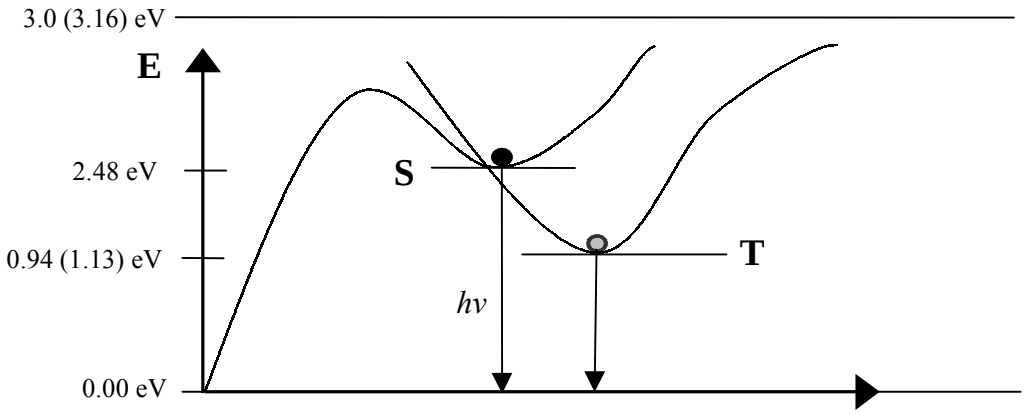


of a given excited system normally lies lower than the singlet state, the luminescence energy due to the triplet exciton should be considerably smaller than the band-gap width. According to the experimental data, the band-gap width in $BaTiO_3$ and $SrTiO_3$ crystals is around 3.0 eV[16] and 3.16 eV,[8] respectively. The observed green luminescence of 2.48 eV[8] in $SrTiO_3$ is very close to this magnitude. Therefore, we expect the green luminescence to occur due to the singlet exciton annihilation as it is shown in Fig. 2. Meantime, the triplet exciton may contribute to the photodegradation process of the material rather than in the emission of green light since the magnitude of its luminescence energy, 0.94 eV for $BaTiO_3$ and 1.13 eV for $SrTiO_3$, falls within the infrared spectrum.

## 4. CONCLUSIONS

The developed for crystals quantum-chemical approach has been applied to study the triplet state of exciton in tetragonal $BaTiO_3$ and $SrTiO_3$ crystals. The structural, electronic and optical properties of the triplet exciton are investigated in detail for both materials. The obtained geometry and the electronic structure of triplet excitons in these crystals are different. The model of the so-called Mott-Wannier exciton, which normally occurs in ionic crystals, describes firmly our results on the exciton geometry of the $BaTiO_3$. However, the triplet exciton in the $SrTiO_3$ lattice resembles characteristics of the two limiting approximations Frenkel and Mott-Wannier. For the $BaTiO_3$, the electron part is well localized on one of the Ti atoms while the hole resonances among three neighboring oxygens. The inter-particle distance is calculated to be equal to 7.0 Å. Meanwhile, in the $SrTiO_3$, the electron and the hole are well localized on Ti and O atoms, respectively, with inter-particle distance equal to 2.14 Å. In both perovskite-type crystals, the obtained atomic displacements within the defective region and electronic charge density re-distribution point to a strong crystalline lattice polarization around the defect. Furthermore, in the $BaTiO_3$ lattice, the exciton-induced dipole moment is opposite to the existing ferroelectric polarization, thus leading to the loss of bulk ferroelectricity in the material. The ΔSCF calculated luminescence energy, 0.94 eV for $BaTiO_3$ and 1.13 eV for $SrTiO_3$, falls within the infrared spectrum. This implies that the experimentally determined luminescence energy of photo-excited state annihilation in the tetragonal $SrTiO_3$ crystal, 2.48 eV,[8] apparently corresponds to the de-excitation of singlet state excitons in this material.

## REFERENCES

1. R. W. G. Wyckoff, *Crystal Structures*, Interscience, New York, 1960.

2. J. Feinberg, D. Heiman, A. R. Tanguay Jr., and R. W. Hellwarth, “Photorefractive effects and light-induced charge migration in barium titanate,” *J. Appl. Phys.* **51**, pp. 1296-1305, 1980.
3. E. Krätzig, F. Welz, R. Orlowski, V. Doormann , and M. Rosenkranz, “Holographic storage properties of $BaTiO_3$,” *Solid State Commun.* **34**, pp. 817-819, 1980.
4. D. Rytz, B. A. Wechsler, M. H. Garrett , C. C. Nelson, and R. N. Schwartz, “Photorefractive properties of $BaTiO_3$:Co,” *J. Opt. Soc. Am. B* **7**, pp. 2245-2254, 1990.
5. D. Balzar, H. Ledbetter, P. W. Stephens, E. T. Park, and J. L. Routbort, "Dislocation-density changes upon poling of polycrystalline $BaTiO_3$," *Phys. Rev. B* **59**, pp. 3414-3420, 1999.
6. P. Sánchez and A. Stashans, "Computational study of structural and electronic properties of superconducting La-doped $SrTiO_3$," *Phil. Mag. B* **81**, pp. 1963-1976, 2001.
7. K. A. Müller and H. Burkard, "$SrTiO_3$: An intrinsic quantum paraelectric below 4 K," *Phys. Rev. B* **19**, pp. 3593-3602, 1979.
8. T. Hasegawa, M. Shirai, and K. Tanaka, "Localizing nature of photo-excited states in $SrTiO_3$," *J. Luminescence* **87-89**, pp. 1217-1219, 2000.
9. A. Shluger and E. Stefanovich, "Models of the self-trapped excitons and nearest-neighbor defect pair in $SiO_2$," *Phys. Rev. B* **42**, pp. 9664-9673, 1990.
10. R. I. Eglitis, E. A. Kotomin, and G. Borstel, "Quantum chemical modelling of electron polarons and excitons in $ABO_3$ perovskites," *J. Phys.: Condens. Matter* **12**, pp. L557-L562, 2000.
11. E. V. Stefanovich, E. K. Shidlovskaya, A. L. Shluger, and M. A. Zakharov, “Modification of the INDO calculation scheme and parametrization for ionic crystals,” *Phys. Status Solidi (b)* **160**, pp. 529-540, 1990.
12. A. Stashans and H. Pinto, "Hole polarons in pure $BaTiO_3$ studied by computer modeling," *Int. J. Quant. Chem.* **79**, pp. 358-366, 2000.
13. H. Pinto and A. Stashans, "Quantum-chemical simulation of Al- and Sc-bound hole polarons in $BaTiO_3$ crystal," *Comput. Mater. Sci.* **17**, pp. 73-80, 2000.
14. A. Stashans and H. Pinto, "Analysis of radiation-induced hole localisation in titanates," *Rad. Measurements* **33**, pp. 553-555, 2001.
15. A. Stashans, "Quantum-chemical studies of free and potassium-bound hole polarons in $SrTiO_3$ cubic lattice," *Mater. Chem. Phys.* **68**, pp. 126-131, 2001.
16. L. M. Prócel, F. Tipán, and A. Stashans, "Mott-Wannier excitons in the tetragonal $BaTiO_3$ lattice," *Int. J. Quant. Chem.*, in press, 2002.
17. A. Stashans and F. Vargas, "Periodic LUC study of F centers in cubic and tetragonal $SrTiO_3$," *Mater. Lett.* **50**, pp. 145-148, 2001.
18. A. Stashans and P. Sánchez, "A Theoretical study of La-doping in strontium titanate," *Mater. Lett.* **44**, pp. 153-157, 2000.
19. F. Erazo and A. Stashans, "Quantum-chemical studies of Nb-doped $CaTiO_3$ crystal," *Phil. Mag. B* **80**, pp. 1499-1506, 2000.
20. E. Patiño and A. Stashans, "Structural and electronic effects in $BaTiO_3$ due to the Nb doping," *Ferroelectrics* **256**, pp. 189-200, 2001.
21. E. Patiño, A. Stashans, and R. Nieminen, "Quantum chemical study of effects produced by Nb- and La-doping in $BaTiO_3$," *Key Engin. Mater.* **206/213**, pp. 1325-1328, 2002.
22. A. Stashans, C. Zambrano, A. Sánchez, and L. M. Prócel, "Structural properties of $PbTiO_3$ and $PbZr_xTi_{1-x}O_3$: a quantum-chemical study," *Int. J. Quant. Chem.* **87**, pp. 145-151, 2002.
23. A. Stashans, F. Erazo, J. Ortiz, and P. Valverde, "Oxygen-vacancy defects on the $SrTiO_3$ (001) surface: a quantum-chemical study," *Phil. Mag. B* **81**, pp. 1977-1988, 2001.
24. A. Stashans and S. Serrano, "A quantum-chemical study of polar $SrTiO_3$ (110) surface and oxygen-vacancy defects therein," *Surf. Sci.* **497**, pp. 285-293, 2002.
25. R. I. Eglitis, E. A. Kotomin, and G. Borstel, "Quantum chemical modelling of electron polarons and charge-transfer vibronic excitons in $BaTiO_3$ perovskite crystals," *J. Phys.: Condens. Matter* **14**, pp. 3735-3741, 2002.

* Correspondence: Email: sauleskalns@yahoo.com; Fax:+593-2-2401583